Pulsed Field Gradient NMR Studies of Translational Diffusion in Cylindrical Surfactant Aggregates

Fredrik Joabsson,* Magnus Nydén, Per Linse, and Olle Söderman

Department of Physical Chemistry 1, Center for Chemistry and Chemical Engineering, Lund University, P.O. Box 124, S-221 00 Lund, Sweden

Received: June 10, 1997; In Final Form: August 26, 1997[⊗]

The motion of molecules captured inside the rods of hexagonal phases of several water-in-oil (w/o) and oil-in-water (o/w) didodecyldimethylammonium sulfate/bromide−hydrocarbon−water systems has been measured by using the pulsed field gradient (PFG) NMR technique. The self-diffusion of hexadecane and dodecane in the case of o/w aggregates, as well as water in the case of w/o aggregates, has been investigated at different diffusion times. It was found that only for the oil-in-water aggregates could the true self-diffusion coefficients for translational motion along the cylinder axis be obtained, on account of the rms displacement during the NMR time scale of the oil molecules being smaller than the surfactant aggregate microdomains. The results show that the self-diffusion coefficient for hexadecane is reduced by a factor of roughly 10, while for dodecane only by a factor of roughly 5, as compared to the respective bulk self-diffusion coefficient. Possible reasons for the reductions are discussed.

Introduction

Lyotropic hexagonal liquid crystalline phases consist of cylindrical aggregates, which are built up by surfactants and packed in a two-dimensional array. They can be of either the water-in-oil (w/o) or the oil-in-water (o/w) type, the latter type usually referred to as normal and the former as reversed.

An interesting question that can be raised about hexagonal phases is to what extent the dynamic properties of the molecules captured inside the hexagonal rods are affected by the size of the aggregates. It has been presumed, not without controversy, that the properties of hydrocarbons inside surfactant aggregates of the normal hexagonal type are very similar to those in the pure hydrocarbon. However, the radius of the core of these systems is often close to the size of the solubilized molecule, which implies that contact between a single hydrocarbon molecule and the surfactant has to be frequent. Since the surfactant translational motion is much slower than that of the hydrocarbon, the self-diffusion coefficient of the hydrocarbon is expected to be reduced, due to wall friction and/or penetration into the surfactant tail region, as compared with the corresponding bulk diffusion coefficient.

The water diffusion coefficient in a w/o system is not expected to be reduced to the same extent as the corresponding hydrocarbon case, since the aggregate palisade layer is less penetrable to a water molecule than a hydrocarbon. On the other hand, one would expect some degree of interaction between the water molecules and the surfactant headgroups with counterions that has to be taken into account.

The evaluation of true self-diffusion coefficients requires the aggregate microdomain size to be large compared to the average translational distance traveled by the core molecules on the NMR time scale. Experimentally, this restricts the measurements to be performed on systems where the microdomains are on the order of micrometers or larger.

Ternary systems with the double-chained surfactants didodecyldimethylammonium bromide (DDAB) and its sulfate analogue (DDAS) have previously been investigated,[1−4] and it has been shown that the aggregate curvatures of these systems depend strongly on the type of counterion used. When sulfate is present as counterion, the curvatures are normal, i.e., bending toward the oil, while in the case of bromine as counterion the reversed behavior dominates, i.e., bending toward water. The reason for this behavior is still not fully understood, but one suggestion is based on differences in the counterion hydration shells. The DDAB−dodecane−water system forms a reverse hexagonal phase in the region around 60% w/w water and 15% w/w oil, while the DDAS−dodecane−water system exhibits a normal hexagonal phase with water as continuous phase around 30−38% w/w water and 20−30% w/w oil (cf. Figure 1). As a consequence, one can study both water and oil self-diffusion in hexagonal rods in DDAX systems, provided the size requirement of the microdomains is fulfilled.

NMR self-diffusion measurements of lyotropic liquid crystalline systems have previously been performed on cubic and lamellar phases, with varying success.[5−8] The purpose of this work has been to measure the self-diffusion inside the hexagonal rod of the dispersed phase, with the intention of obtaining information about reduction of the diffusion coefficient due to the wall friction and the hexagonal microdomain size and structure.

Theoretical Background

The NMR pulsed field gradient (PFG) technique provides a tool for measuring molecular motion (for general reviews of the method, see refs 9−12). Self-diffusion coefficients of molecules in solution can be measured with PFG spin-echo experiments. In this study we have used the stimulated spin-echo pulse sequence, which has several advantages over the basic 90_x-180_y sequence. In a stimulated echo, the signal appearing at the echo time is mainly affected by T_1 relaxation processes rather than T_2. In many cases this makes it possible to follow diffusion on longer time scales, since T_1 often is longer than T_2 for nuclei in systems where the correlation times for tumbling and rotation are long. Also, a T_2-dependent time delay, τ, in the stimulated echo makes it possible to separate out fast relaxating (T_2) components from the spin echo.

The PFG technique has mostly been applied to isotropic systems for the determination of component resolved self-

[⊗] Abstract published in *Advance ACS Abstracts,* October 1, 1997.

S1089-5647(97)01890-7 CCC: $14.00

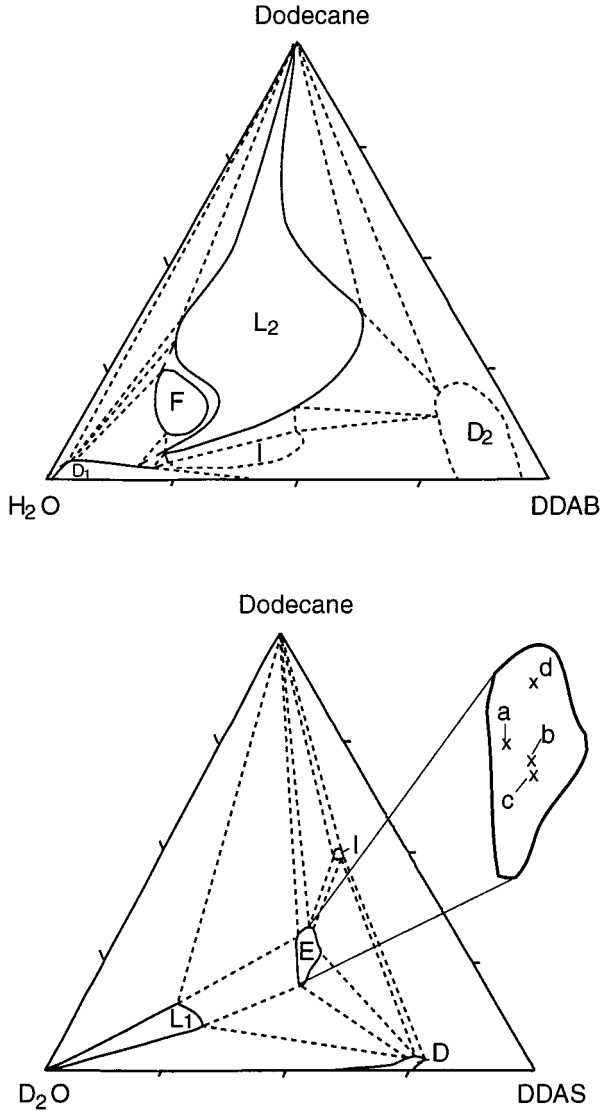

Figure 1. Ternary phase diagram (by weight) for the DDAB−dodecane−water system (upper) and for the DDAS−dodecane−water system (lower). An enlargement of the DDAS phase diagram shows the prepared samples. Point a corresponds to sample 6, b to 3 and 5, c to 4, and d to 7. The phase diagrams are redrawn from refs 4 and 2, respectively. The hexagonal phase of the DDAB system was found to be slightly shifted off the water corner compared to the drawn phase diagram.

diffusion coefficients. With respect to the limitations of the technique, the application window of diffusion coefficients (nonrestricted motion) lies in the range $10^{-9}-10^{-15}$ m^2 s^{-1}. When applied to restricted systems, for instance one-dimensional diffusion in randomly distributed rods, this window becomes more narrow, due to the weak echo attenuation of the microdomains where only motion perpendicular to the applied gradient field is allowed.

Theoretical expressions for the anisotropic diffusion in lamellar and hexagonal systems have been derived by Callaghan and Söderman[5] (see also Callaghan[12]). In the hexagonal case it was assumed that the diffusion perpendicular to the director is insignificant compared to the parallel diffusion. It is easy to convince oneself that this is a realistic assumption. Take for example the normal hexagonal case with DDAS−water−dodecane. Previous studies have shown that the radius of the rod is roughly 30−40 Å.[1,2] The thickness of the surfactant layer in the DDAS−water−dodecane hexagonal system is approximately 11 Å, calculated from ref 1, which for DDAS is equivalent to a palisade layer thickness of $l \approx 0.65 l_c$, where l_c is the tail length. This leaves a radius of approximately 20−30 Å for the oil cylinder. This length should be compared to the average distance traveled by a molecule during the time of the measurement. The root-mean-square displacement along an arbitrary coordinate axis is equal to

$$\langle x^2 \rangle^{1/2} = (2D\Delta)^{1/2} \tag{1}$$

where D and Δ are the diffusion coefficient of the molecule and diffusion time, respectively. Since the time scale of NMR diffusion measurements lies in the range 20−1000 ms and the diffusion coefficients in the order $10^{-9}-10^{-11}$ m^2 s^{-1}, displacements are on the micrometer scale. This implies, provided wall penetration can be excluded, that nonparallel diffusion in the rods is negligible.

The theoretical expression for the echo attenuation in the case of free nonrestricted diffusion is given by the well-known Stejskal−Tanner expression:[13]

$$E(q) = \exp[-4\pi^2 q^2 (\Delta - \delta/3) D] \tag{2}$$

where q is $\gamma g \delta / 2\pi$, γ is the magnetogyric ratio, g is the gradient pulse strength, and δ is the duration of the gradient pulse. $\Delta - \delta/3$ is often referred to as the effective diffusion time, where Δ is the time between the leading edges of the gradient pulse.

In hexagonal systems the motion of the molecules captured inside the rods is restricted as discussed above, which implies that the Stejskal−Tanner expression has to be modified. Since the motion along the rod director is unrestricted, whereas the motion perpendicular to the director is negligible, the motion can be considered as one-dimensional. Provided the orientations of the microdomains are randomly distributed and their symmetry axis long compared to the average translational displacement during Δ, the echo attenuation in this case can be derived by powder averaging the nonrestricted one-dimensional echo attenuation expression[5,12,14]

$$E(q) = \int_0^1 \exp[4\pi^2 q^2 (\Delta - \delta/3) D x^2] \, dx \tag{3}$$

where $x = \cos\theta$ with θ being the polar angle between an individual rod director and the applied gradient field direction. The integral in eq 3 can be evaluated, and the equation that is used in the fitting procedures in this work is

$$E(q) = (16\pi q^2 (\Delta - \delta/3) D)^{-1/2} \operatorname{erf}[2\pi q ((\Delta - \delta/3) D)^{1/2}] \tag{4}$$

where erf is the error function.

Computer Simulation

The validity of eq 4 requires that the length of the microdomains in the rod director direction are long on the displacement distance scale exploited by the NMR diffusion experiments. When rms displacements approach the same order as the length of the microdomains, deviations from eq 4 are expected. To investigate this regime, we have performed simulations of the Brownian motion of spin-bearing molecules in long chains of connected rods (see the EEICR model below). The angle between two adjacent rod segments, α, is randomly distributed between zero and a maximum value, α_{max}, while the length of the segments, l, is held fixed. New chains of rods are produced for every molecule trajectory that is followed, and the starting position of the molecule is in the middle segment. As already discussed above, it is only one-dimensional diffusive motion that has to be considered inside the rods.

The algorithm for generating the molecular motion is described as follows: A molecule performs a Brownian displacement, $R(\Delta t)$, along the rod during the time, Δt. The

TABLE 1: Compositions of the Samples in % w/w

sample	m_{DDAS}	m_{DDA}	$m_{dodecane}$	$m_{hexadecane}$	m_{D_2O}	temp treated[a]
1		25.9	15.8		58.3[b]	
2		25.9	15.8		58.3[b]	x
3	41.9		25.1		33.0	
4	41.9		24.0		34.0	x
5	41.9			25.0	33.0	
6	39.8			26.2	33.9	
7	39.6			30.1	30.3	x

[a] See text for details. [b] The samples contain D_2O, but the weights are recalculated to H_2O in order to be comparable with the phase diagram of DDAB−dodecane−water.

random displacement is taken from a Gaussian probability distribution function with the statistical properties

$$\langle R(\Delta t)\rangle = 0 \quad \langle R(\Delta t)^2\rangle = 2D\Delta t \tag{5}$$

where D is the self-diffusion coefficient of the molecule. If the new position of a molecule after the displacement is outside the original rod segment, the molecule enter the adjacent rod segment. The number of rods in a chain is sufficiently large that a molecule never exits the chain of rods during the random motion.

The simulated phase shift, ϕ, caused by the diffusion of molecule i is

$$\phi_i = \gamma g[\int_{t_1}^{t_1+\delta} z_i(t)\,\mathrm{d}t - \int_{t_1+\Delta}^{t_1+\Delta+\delta} z_i(t)\,\mathrm{d}t] \approx \gamma g[\sum_{j=a}^{a+b} z_{i,j} - \sum_{j=a+c}^{a+b+c} z_{i,j}](\Delta t) \tag{6}$$

where t_1 is the time of the application of the first gradient pulse. In the discretization procedure, $z_j = z(t)$ and $j = a$, b, and c for $t = t_1$, d, and Δ, respectively, are used. The echo attenuation is subsequently calculated by using the relation

$$E = \int_{-\infty}^{\infty} P(\phi)\cos(\phi)\,\mathrm{d}\phi \approx (1/\mathrm{N})\sum_{i=1}^{N}\cos\phi_i \tag{7}$$

where the phase shift distribution $P(\phi)$ is obtained by simulating N spin trajectories.

Experimental Section

Materials. DDAB was obtained from Tokyo Kasei and used without further purification. DDAS was prepared by ionic exchange (Dowex 1 ionic form: hydroxide dry mesh 20−50) starting from DDAB.[1,2] An excess of ion exchanger was washed 10 times with Millipore water and stirred with 1 M NaOH for 2 h, whereupon it was carefully rinsed with several portions of Millipore water. DDAB was added to the mixture of ionic exchanger and Millipore water and stirred vigorously until all DDAB was dissolved. The solution was filtered, and the ion exchanger was washed with small portions of Millipore water until the filtrate was neutral. The filtrate was neutralized with 1 M sulfuric acid, and the resulting precipitate was separated from the water phase by freeze-drying. The DDAS was additionally purified by recrystallization from ethyl acetate. The yield was better than 90%. Dodecane and hexadecane were obtained from Merck and Fluka, respectively, and D_2O was supplied by Dr. Glaser AG.

Sample Preparation. Samples were prepared by weighing the components and mixing until homogeneity. All sample compositions are given in Table 1. The samples were transferred, with a syringe, to 4 or 5 mm NMR tubes that were flame-sealed. Samples 2, 4, and 7 were treated by a temperature decrease procedure, in which they were placed in a hot water bath and the temperature was slowly lowered from 70 to 25 °C over 70 h by using a frequency modulator. At 70 °C the reversed hexagonal phase of the DDAB−dodecane−water system had disappeared, and instead an isotropic solution was obtained. The purpose of the temperature treatment was to obtain larger microdomains of hexagonal rods when re-forming the hexagonal phase from the isotropic solution very slowly. In the case of DDAS−dodecane−water and DDAS−hexadecane−water, the hexagonal phase seemed to be almost unchanged at 70 °C compared to 25 °C. Despite this fact, differences in the visual (as observed between crossed polaroids) appearance of the samples could be observed. The compositions of the samples are shown in Table 1. All samples were kept at 25 °C after preparation.

Self-Diffusion Experiments. Measurements of the self-diffusion were performed on a Bruker 200 MHz NMR spectrometer using the pulsed field gradient (PFG) spin-echo technique. ^{1}H was observed, and the stimulated spin-echo pulse sequence was used for all measurements. The temperature was kept at 25 °C. The diffusion time, Δ, was varied between 50 and 1000 ms, while the gradient pulse length, δ, was varied between 2 and 5 ms. The time between the first two 90° rf pulses was kept constant at 10 ms for all rod diffusion measurements to make sure that no signal contribution arising from the surfactants was present. The DDAS T_2 value of a deuterated hexadecane hexagonal phase sample was measured and showed that the relaxation of the surfactant was very fast ($T_2 < 1$ ms). For the case of oil diffusion (samples 3−7) the gradient pulse strength, g, was increased stepwise to a maximum of 4.8 T/m for the shorter diffusion times (50 and 100 ms) and 4.4 T/m for the longer diffusion times. Twenty-six steps of g were used, where the first 10 points were collected with a shorter spacing in order to obtain a more accurate determination of the steeper part of the echo attenuation. For the water-in-oil samples (samples 1−2) g was increased in 20 steps to the same maximum values as for the oil-in-water samples. In all measurements 16 scans were accumulated, to perform adequate phase cycling and to obtain a satisfactory signal-to-noise level. The diffusion coefficients were calculated by fitting an expression for echo decay in an infinitely long rod (cf. eq 4) to the raw NMR data by means of a nonlinear least-squares fitting procedure based on the Levenberg−Marquardt method. In the case of dodecane both the methyl and methylene intensity decay could equivalently be used in the fitting procedure. For hexadecane, only the methyl peak was used, since residual dipolar couplings of the methylene protons of hexadecane made the data evaluation more complicated (as evidenced by quadrupolar splittings of the oil peak in the 90° deuterium spectrum).

Computer Simulations. The simulations were performed by using a modified version of the spin-echo attenuation computer simulation program, PGSE. The diffusion time was set to 700 ms and the diffusion coefficient to 5×10^{-11} m^2 s^{-1}, and the gradient pulse length was applied in 10 steps from 0.25 to 2.5 ms. The gradient pulse strength g was set to two different values, 1.408 and 7.039 T m^{-1}, for the purpose of collecting more points in the beginning of the echo attenuation. The number of spin trajectories used was 3×10^4 in order to obtain satisfactory statistical accuracy. The intersegmental maximum angle α_{max} (see Figure 6 and under Computer Simulations section) was varied between 20° and 60°, and the segment length, l, was changed from 0.1 to 10 μm for each angle.

Results and Discussion

Reversed Hexagonal Phase. The DDAB−water−dodecane system forms a reverse hexagonal phase in a small area around

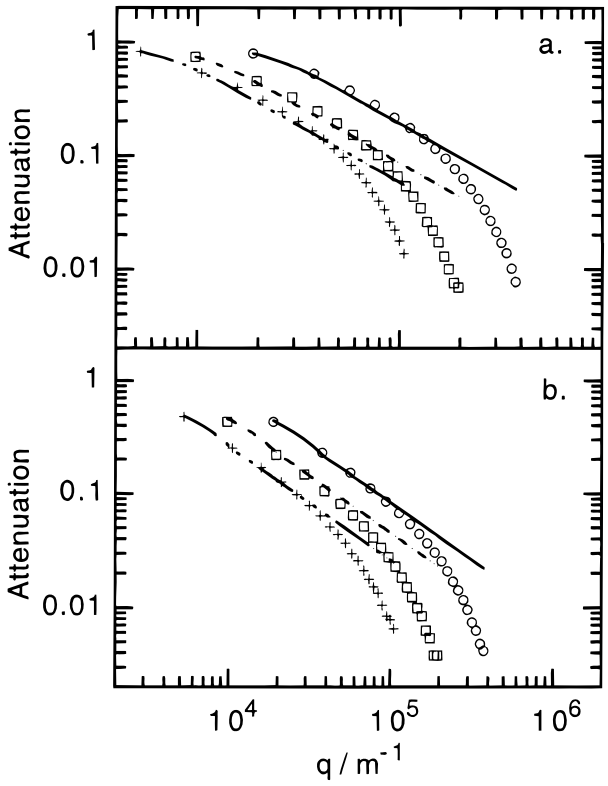

Figure 2. Echo attenuations of the reversed hexagonal phase samples. (a) shows the echo attenuation of sample 1, and (b) shows the same for sample 2 (treated by the temperature decrease procedure). (○), (□), and (+) shows the experimental data when 100, 400, and 1000 ms diffusion time was applied. The solid and dashed lines are the corresponding fittings to eq 4.

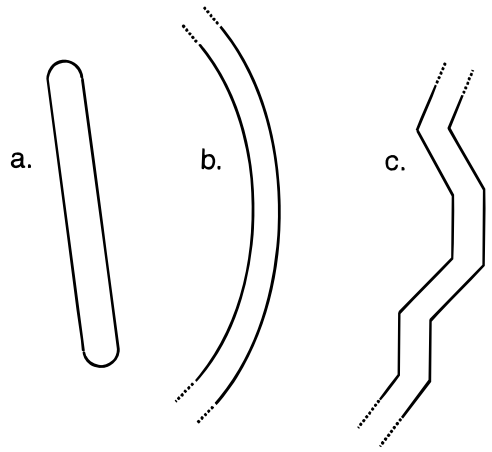

Figure 3. Examples of simple models that could be used for describing the echo attenuation in systems where eq 4 fails, i.e., in the region when the rods no longer can be considered as infinite long and straight on the NMR time scale: (a) end-capped rods, (b) bent rods, and (c) end-to-end interconnected rods, EEICR model. Compared to a true hexagonal system the radial length scale is more enlarged than the axial.

25−60−15% w/w DDAB−H_2O−C_{12}, as mentioned above (see Figure 1). Since water is only sparingly soluble in dodecane, practically all water is found in the interior of the rods. The interface between the surfactant monolayer and the innermost core of water and bromium ions is most likely rather sharp; i.e., water molecules do not penetrate into the surfactant region. The water diffusion coefficient in this system is therefore expected to be close to the diffusion coefficient for free water molecules, D_0. However, one has to remember that it is not pure water inside the rods, but a highly concentrated ionic solution of the surfactant bromide counterions (of order 1 M),

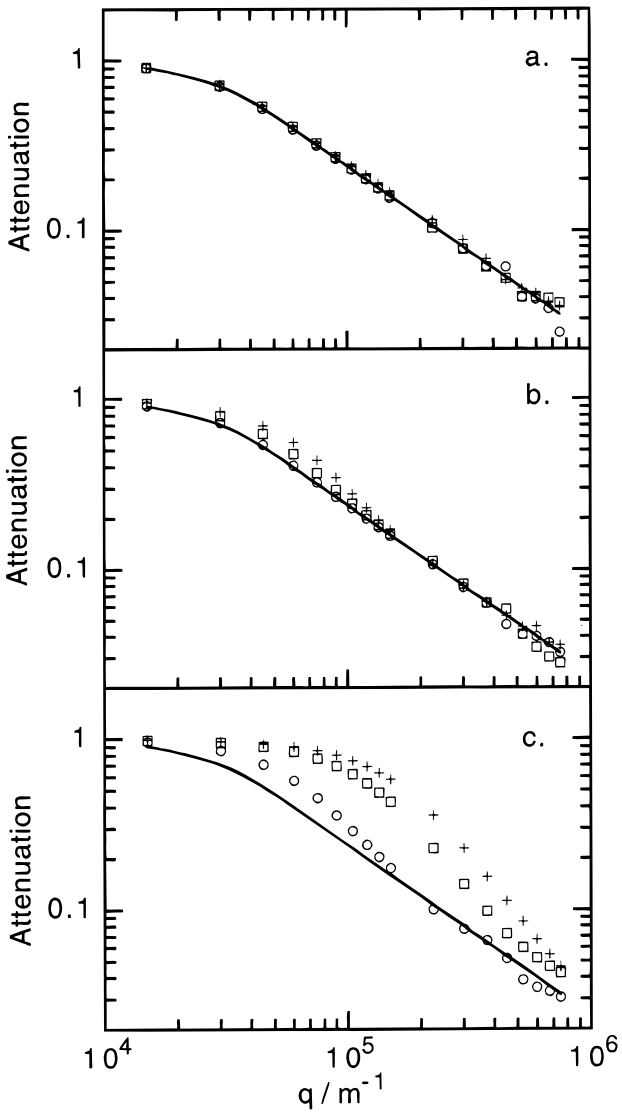

Figure 4. Simulated echo attenuations showing the intersegment angular and segment length dependence. (a), (b), and (c) show attenuations of three different segment lengths 10, 1, and 0.1 μm, respectively. (○), (□), and (+) show data from simulations with a maximum intersegment angle of 20°, 45°, and 60°. The solid lines show the infinite segment length limit. The simulation input parameters was $\Delta = 700$ ms, $d = 0.25-2.5$ ms, and $D = 5 \times 10^{-11}$ m^2 s^{-1}.

which in fact is going to alter the diffusion coefficient from that of pure water.

NMR self-diffusion measurements of the DDAB−water−dodecane system are presented in Figure 2. The results show that the water molecules diffuse in a non-Gaussian manner, and as a consequence the experimental data cannot be fitted to the analytical expression given by eq 4. The sample exposed to the temperature decrease procedure (sample 2) showed no large differences in diffusion behavior. This sample did not completely reenter into the hexagonal phase area but ended up in the two-phase region between the hexagonal and microemulsion phase areas. The diffusion measurements were performed only on the part of the samples that was hexagonal.

As discussed above, the echo attenuation of a PFG spin-echo measurement starts to deviate from the eq 4 shape when the rod length is close to the rms displacement (cf. eq 1). If this is the case, several possible explanations may be invoked to account for the deviations, a few of which are schematically illustrated in Figure 3. The rods could be capped at the ends, or the rods could be bent with the degree of bending described by a persistence length. Other cases could be a system where

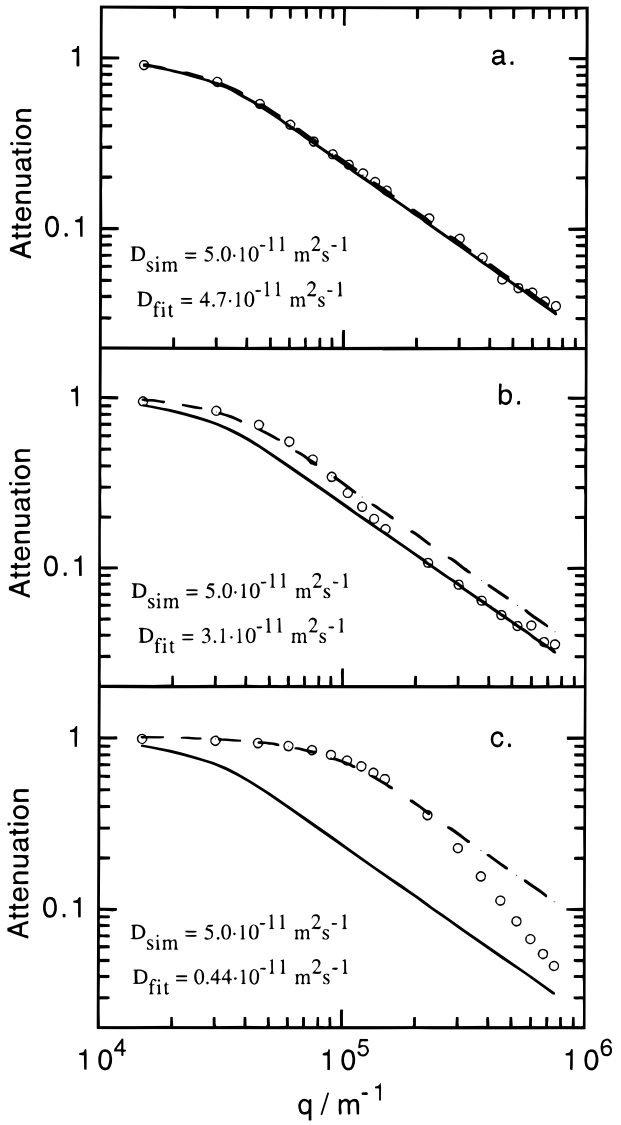

Figure 5. Fittings of simulation data with a maximum intersegment angle of 60°. (a), (b), and (c) show attenuation plots of three different segment lengths, 10, 1, and 0.1 μm, respectively. The solid lines represent the infinite segment length limit, while the dashed lines show the results of fitting eq 4 to the data. The input value of D in the simulation and the result of the fit are included in the figures.

the walls of the cylinders have a finite permeability to the molecules inside the rods or a system where the microdomains face each other on the short ends of the packed rods, connecting two individual rods of adjacent microdomains in an end-to-end manner (the model of end-to-end interconnected rods, referred to as the EEICR model). All these proposals can be modeled by computer simulations, but we have focused only on the last one. Figure 4 shows the dependence of the simulated echo attenuation when the segment length approaches the rms displacement (rms = 8.4 μm) for different maximum permitted intersegment angles (20°, 45°, and 60°). It is notable that the echo attenuation does not become considerably affected before the segment length becomes of the order of 10% of that of the rms displacement. At this and shorter segment lengths the echo attenuation shows a large angle dependence. If the simulated echo attenuations are fitted to the analytical expression for rods of infinite length, eq 4, large errors in the diffusion coefficients are obtained (Figure 5).

It appears that the simulated echo shown in Figures 4 and 5 and the experimental echo attenuation of the water displacement in the reversed hexagonal phases shown in Figure 2 have similar curve shapes. The EEICR model used in the computer simulations can hence possibly account for the echo attenuation behavior in these systems. To illustrate the system as such, two representative computer generated chains of rods (with an overall end-to-end distance close to the mean value) is projected in Figure 6.

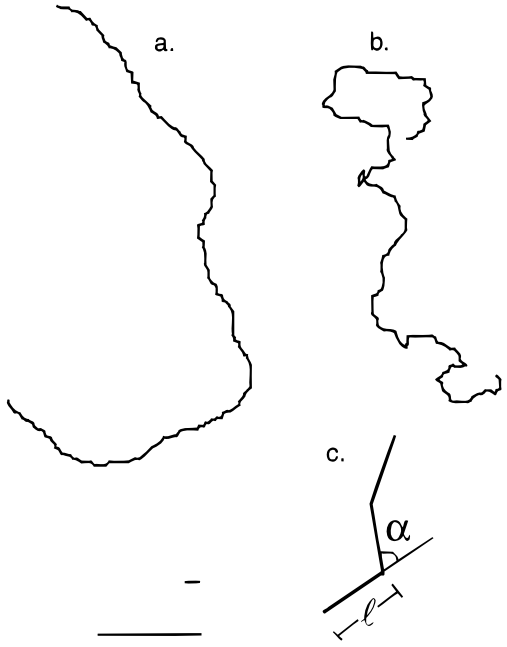

Figure 6. Two representative (an overall end-to-end distance close to the mean value) chain of rods projected in the plane, illustrating the EEICR model used in the computer simulation. (a) represents a chain with a maximum intersegment angle of 20°, while (b) shows a chain 60° maximum angle. The chains consists of 100 segments each, and the short bar at the bottom shows the length of a segment (the long bar shows the length of 10 fully stretched segments). (c) shows the intersegment angle, α, and segment length, l, parameters. α is randomly distributed between zero and a maximum value, α_{max}, while l is held fixed.

In conclusion, no diffusion coefficient of water could be obtained, on one hand due to insufficient size of the microdomains in the DDAB−water−dodecane system and on the other the coarseness of the computer simulation model used, making it inapplicable to diffusion coefficient determination.

Normal Hexagonal Phase. The bulk self-diffusion coefficients of dodecane and hexadecane are measured and will later be referred to as D_0 (which hydrocarbon that is referred to will be evident from the context). The results from these measurements are $D_{0,\text{dodecane}} = (8.81 \pm 0.03) \times 10^{-10}$ m^2 s^{-1} and $D_{0,\text{hexadecane}} = (4.62 \pm 0.04) \times 10^{-10}$ m^2 s^{-1}, in reasonable agreement with literature data.

The DDAS−water−dodecane system as well as the DDAS−water−hexadecane system forms a normal hexagonal liquid crystalline phase around 30−38% w/w water and 20−30% w/w oil, with the oil in the interior of the rods and water as continuous medium. This phase forms with several *n*-alkanes having at least 10 carbons.[1] For *n*-alkanes with fewer carbons the phase is not formed, presumably on account of penetration effects of oil into the surfactant palisade layer. As a rule of thumb, it appears that, with alkane chain lengths longer than that of the surfactant, only minor penetration of the oil into the surfactant tail region occurs.[15,16]

Figure 7a shows the echo attenuation of a sample with dodecane (sample 3), and Figure 7b shows the corresponding appearance for a sample exposed to the temperature decrease procedure (sample 4). The data have been fitted to eq 4, and it is clear that the model with rods of infinite length gives a better representation for the temperature treated sample than for the nontreated sample.

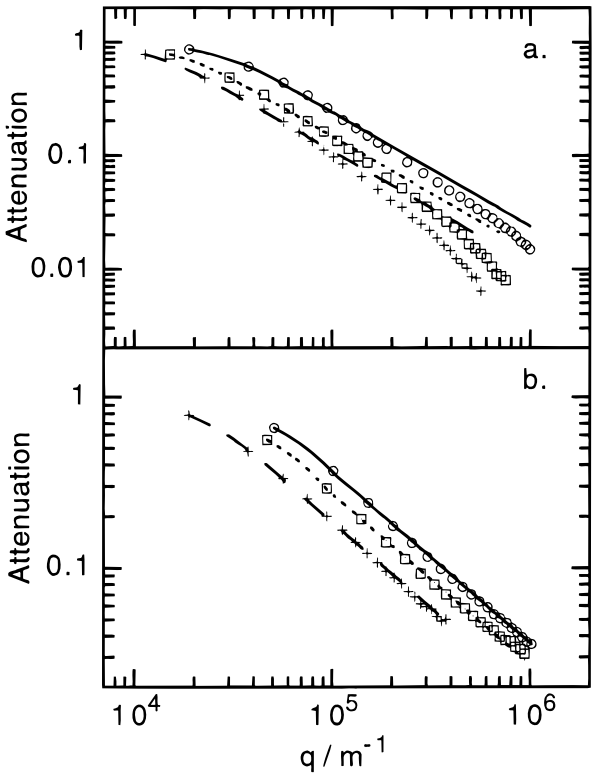

Figure 7. Echo attenuation plots from normal hexagonal phase dodecane samples. (a) shows sample 3, not treated by the temperature decrease procedure, while (b) shows sample 4 exposed to the temperature treatment. (○), (□), and (+) show the experimental data when 100, 400, and 1000 ms diffusion time was applied. The solid and dashed lines represent the corresponding fitting to eq 4. The dodecane self-diffusion coefficients obtained from the fit are (in turn 100, 400, and 1000 ms) $(3.6 \pm 0.2) \times 10^{-10}$, $(2.3 \pm 0.2) \times 10^{-10}$, and $(1.7 \pm 0.2) \times 10^{-10}$ m^2 s^{-1} for sample 3 and $(2.6 \pm 0.6) \times 10^{-10}$, $(2.0 \pm 0.8) \times 10^{-10}$, and $(2.0 \pm 0.9) \times 10^{-10}$ m^2 s^{-1} for sample 4.

In the case of the normal hexagonal phase constituted of DDAS−water−hexadecane, the data from samples 5 and 6 could be satisfactorily fitted to eq 4 without exposing the samples to the temperature decrease procedure (see Figure 8). One sample (sample 7) was temperature treated but showed no improvement in the fitting procedure (data not shown).

The combined data from five different Δ values of samples 4−6 (between 50 and 1000 ms) was analyzed by using a global fitting procedure, in which a total of 126−130 data points were used. The observed diffusion coefficient for sample 4, $D = 1.92 \times 10^{-10}$ m^2 s^{-1} (as obtained from a global fitting procedure, see Table 2), gives an obstruction factor, $f \approx 0.2$ (the obstruction factor is defined as $f = D/D_0$). For sample 3, D depends on the diffusion time, which implies that the model with rods of infinite length cannot be applied on this sample (Figure 7a). The outcome of this fit was for sample 5, $D = 5.5 \times 10^{-11}$ m^2 s^{-1}, and for sample 6, $D = 6.6 \times 10^{-11}$ m^2 s^{-1}. The values for hexadecane obtained give an obstruction factor, $f \approx 0.12-0.14$. The diffusion coefficients are shown in Table 2.

The echo attenuation outcome in the case of normal hexagonal phase differs from the reversed phase echo attenuation. The experimental data could be fitted to the theoretical expression, eq 4, which implies that the microdomain length has to be close to or longer than the rms displacements. In the dodecane case, the non-temperature-treated sample shows a clear Δ dependence of the observed diffusion coefficient (see Figure 7). This implies that either the microdomain lengths are shorter than the rms displacements and the EEICR model or the other models suggested above may account for the deviation. In the ideal case with rods of infinite length, the steep initial part of the attenuation curve is dominated by the fast phase shift arising from the rods parallel or almost parallel to the field gradient. Let us for comparison consider a case when the rods are pleated or bent. If the rms displacements are longer than the microdomains, the studied molecules will, during the time of the measurement, experience several angles with the field gradient director. This results in a less steep initial part of the attenuation curve and therefore lower observed diffusion coefficients from the longer Δ measurements. In line with this is also the observation that in all cases the experimental data have a faster decay than the fitted curve for high q values. Also in this case it is fruitful to compare the two cases described above. In the

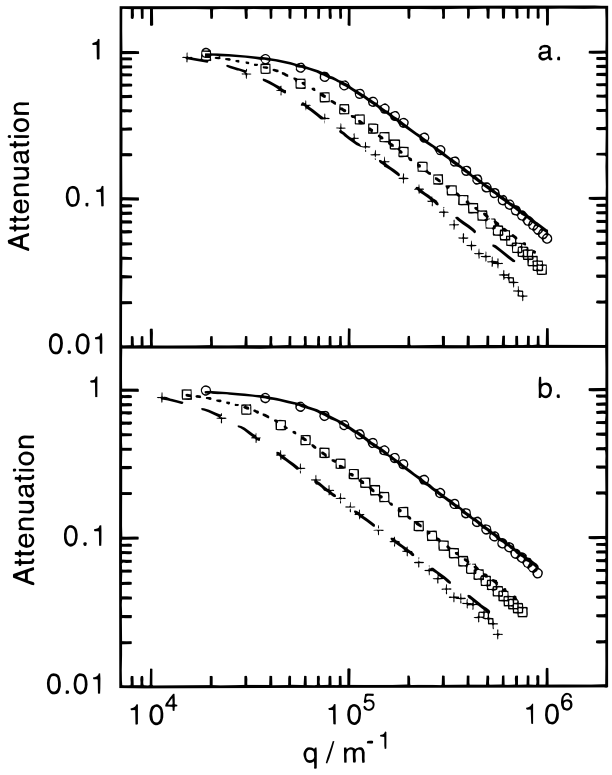

Figure 8. Echo attenuation plots from normal hexagonal phase hexadecane samples. (a) shows sample 5 and (b) shows sample 6. The notations are the same as in Figure 7. The hexadecane self-diffusion coefficients obtained from the fit are (in turn 100, 400, and 1000 ms) $(5.6 \pm 0.1) \times 10^{-11}$, $(5.4 \pm 0.2) \times 10^{-11}$, and $(5.3 \pm 0.2) \times 10^{-11}$ m^2 s^{-1} for sample 3 and $(6.2 \pm 0.2) \times 10^{-11}$, $(6.5 \pm 0.2) \times 10^{-11}$, and $(7.5 \pm 0.1) \times 10^{-11}$ m^2 s^{-1} for sample 4.

TABLE 2: Self-Diffusion Coefficients of Dodecane (Sample 4) and Hexadecane for the Samples Whose Echo Attenuation Curve Could Be Fitted to Eq 4, Obtained from a Global Fitting Procedure; Fits Include Data from up to Six Different Diffusion Time Values between 50 and 1000 ms

		80% confidence interval from MC uncertainty estimation[a]	
sample	$D_{\text{global fit}}/10^{-11}$ m^2 s^{-1}	$D_{\text{err}}/10^{-11}$ m^2 s^{-1}	%
4 (C_{12})	19.2 ± 0.8	0.95	5.0
5 (C_{16})	5.46 ± 0.08	0.40	7.4
6 (C_{16})	6.53 ± 0.08	0.36	5.5
7 (C_{16})	6.2 ± 0.1	0.42	6.8

[a] Experimental data also analyzed by a Monte Carlo uncertainty estimation procedure.[19,20] The statistical uncertainties of the raw echo intensities was initially estimated from the mean of the absolute residuals obtained by the usual Levenberg−Marquardt method. A "new" set of echo attenuation data was produced by adding a Gaussian distributed error, weighted by the initial uncertainty estimation, to each data point. Each new set of echo attenuation data was subsequently fitted to eq 4 by using the Levenberg−Marquardt method. By repeating the procedure 5000 times, an approximately Gaussian-shaped distribution of diffusion coefficients was obtained.

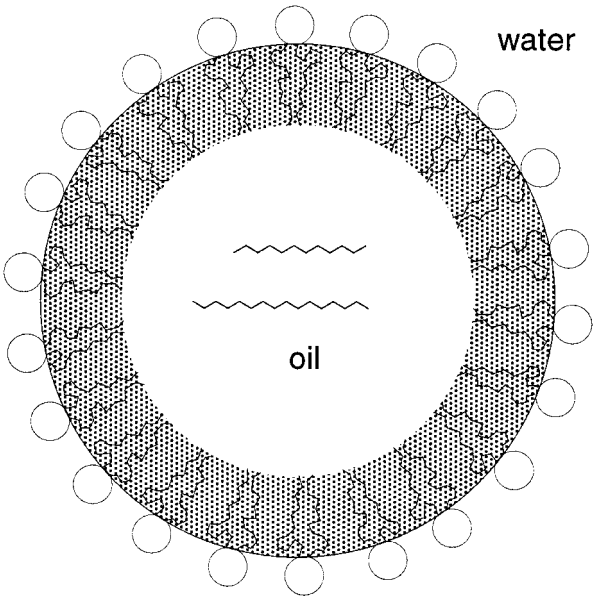

Figure 9. Cross section of a hexagonal rod with the composition corresponding to point (b) in Figure 1. The rod dimensions are calculated from data presented in ref 1, assuming that the hexadecane system has the same radius as the corresponding dodecane system. The pleated lines in the middle of the oil core represent fully stretched dodecane (the shorter one, 18 Å) and hexadecane (the longer line, 23 Å) made to scale. The radius of the oil core is roughly 24 Å, and the surfactant monolayer thickness is about 11 Å (the surfactant tails only considered). No oil penetration into the surfactant monolayer was assumed to occur.

ideal case, this part of the curve obtains its signal contribution from the rods perpendicular to the applied gradient field. As an obvious consequence, the spin-echo signal will die out to a larger extent in the case of pleated or bent rods.

The diffusion coefficient appears to adopt different values depending on where in the hexagonal phase area the samples are prepared, but the differences are small and we do not consider them significant (see Table 2). Previous X-ray measurements of the DDAS−water−dodecane hexagonal phase show that the radius of the rods is dependent on the composition of the sample.[1] It is therefore likely that the hexagonal rods of the dodecane and hexadecane samples 3, 4 and 5, 6 each have different radii. Different radii imply different surface-to-volume ratios, which in all likelihood is an important parameter affecting the diffusion coefficient.

Leaving for a moment the differences in obstruction factor between samples from the same hexagonal phase area aside, we note that there are bigger differences between the dodecane and hexadecane hexagonal phases, hexadecane being the more obstructed in comparison to free diffusion. What does this tell us about the dynamic properties of the core molecules? Intuitively, considering the more pronounced penetration effect of dodecane than of hexadecane, one would have expected the opposite behavior, i.e., dodecane being the more obstructed. The presence of the surfactant tail region would certainly affect the dynamic properties of the core molecules. The surfactant molecules move considerably slower than the hydrocarbons (the lateral diffusion coefficient of DDAC (the chloride analogue of DDAB and DDAS) along a surface has been estimated to $D_{lat} = (0.1-2) \times 10^{-11}$ m^2 s^{-1} [17]), which would affect a core molecule that has found its way into the surfactant tail region, making the diffusion coefficient smaller as compared to D_0.

Considering the oil diffusion in the rod, the hexadecane molecule is longer (fully stretched 23 Å, calculated from $l_c = 3.0 + 1.265n_c$[18]) than the dodecane molecule (18 Å), which statistically would imply that the average hexadecane molecule spends more of its time in contact with the core/palisade layer interface than the average dodecane molecule does. This may account for the more obstructed diffusion manner in case of hexadecane in a hexagonal rod. The cross section of an oil-in-water hexagonal rod is shown in Figure 9, where also one fully stretched molecule of dodecane and hexadecane are drawn to scale.

Conclusions

The motion of molecules captured inside rods of hexagonal phases in the DDAB/DDAS−water−dodecane/hexadecane systems has been investigated. Self-diffusion coefficients of the alkane in the oil-in-water systems could be obtained, provided the rms displacement of the measured molecules was smaller than hexagonal phase microdomain size on the NMR time scale. The diffusion coefficients for dodecane and hexadecane inside the rods of the oil-in-water systems were reduced by approximately a factor of 0.2 and 0.13, respectively, compared to the bulk diffusion coefficients.

For the case of water diffusion in the water-in-oil system, no self-diffusion coefficients could be obtained, which suggested that the microdomain size was smaller than the rms displacements of water molecules on the NMR time scale (on the order of micrometers). Computer simulations of the motion of molecules in chains of interconnected rods were performed, reproducing the trends for a system with smaller microdomains (cf. w/o aggregates), but they could not be used for diffusion coefficient determinations.

Acknowledgment. Björn Håkansson is thanked for his assistance in running the NMR spectrometer used in this work. We also thank Ingegerd Lind for technical assistance and Vijay Rajagopalan for stimulating discussions. This work received financial support from the Swedish Natural Science Foundation (NFR). The NMR spectrometer used was bought with a grant from the Swedish Council for Planning and Coordination of Research (FRN).

References and Notes

(1) Nydén, M.; Söderman, O. *Langmuir* **1995**, *11*, 1537−1545.
(2) Kang, C.; Khan, A. J. *J. Colloid Interface Sci.* **1993**, *156*, 218.
(3) Fontell, K.; Ceglie, A.; Lindman, B.; Ninham, B. W. *Acta Chem. Scand.* **1986**, *A40*, 247.
(4) Skurtveit, R.; Olsson, U. *J. Phys. Chem.* **1992**, *96*, 8640−8646.
(5) Callaghan, P. T.; Söderman, O. *J. Phys. Chem.* **1983**, *87*, 173.
(6) Chidichimo, G.; La Mesa, C.; Ranieri, A.; Terenzi, M. *Mol. Cryst. Liq. Cryst.* **1987**, *150b*, 221−235.
(7) Coppola, L.; La Mesa, C.; Ranieri, A.; Terenzi, M. *J. Chem. Phys.* **1993**, *98*, 5087−5090.
(8) Coppola, L.; Muzzalupo, R.; Ranieri, G. A.; Terenzi, M. *Langmuir* **1995**, *11*, 1116−1121.
(9) Price, B. *Annu. Rep. NMR Spectrosc.* **1996**, *32*, 51−142.
(10) Söderman, O.; Stilbs, P. *Prog. NMR Spectrosc.* **1994**, *26*, 445−482.
(11) Stilbs, P. *Prog. Nucl. Magn. Reson. Spectrosc.* **1987**, *19*, 1−45.
(12) Callaghan, P. T. *Principles of Nuclear Magnetic Resonance*; Oxford University Press Inc.: New York, 1991.
(13) Stejskal, E. O.; Tanner, J. E. J. *J. Chem. Phys.* **1965**, *42*, 288.
(14) Lindblom, G.; Wennerström, H. *J. Quantum Chem.* **1977**, *12*, 153.
(15) Chen, S. J.; Evans, D. F.; Ninham, B. W. *J. Phys. Chem.* **1984**, *88*, 1631.
(16) Gruen, D. W. R.; Haydon, D. A. *Pure Appl. Chem.* **1980**, *52*, 1229.
(17) Söderlind, E.; Björling, M.; Stilbs, P. *Langmuir* **1994**, *10*, 890.
(18) Tanford, C. J. *J. Phys. Chem.* **1972**, *76*, 3020.
(19) Stilbs, P.; Moseley, M. E. *J. Magn. Reson.* **1978**, *31*, 55−61.
(20) Alper, J. S.; Gelb, R. I. *J. Phys. Chem.* **1990**, *94*, 4747.